BBA - Molecular Basis of Disease 1865 (2019) 165524

Contents lists available at ScienceDirect

BBA - Molecular Basis of Disease

journal homepage: www.elsevier.com/locate/bbadis

Tetrahydrobiopterin enhances mitochondrial biogenesis and cardiac contractility via stimulation of PGC1α signaling

Hyoung Kyu Kim[a,1], Jouhyun Jeon[b,1], In-Sung Song[a], Hae Jin Heo[a], Seung Hun Jeong[a], Le Thanh Long[a], Vu Thi Thu[a], Tae Hee Ko[a], Min Kim[a], Nari Kim[a], Sung Ryul Lee[a], Jae-Seong Yang[b], Mi Seon Kang[c], Jung-Mo Ahn[d], Je-Yoel Cho[d], Kyung Soo Ko[a], Byoung Doo Rhee[a], Bernd Nilius[e], Nam-Chul Ha[f], Ippei Shimizu[g], Tohru Minamino[g], Kyoung Im Cho[h], Young Shik Park[i,*], Sanguk Kim[b,*], Jin Han[a,**]

[a] Cardiovascular and Metabolic Disease Center, Inje University, Busan 47392, Republic of Korea
[b] Department of Life Science, POSTECH, Pohang 37673, Republic of Korea
[c] Department of Pathology, Inje University, Busan 47392, Republic of Korea
[d] Department of Veterinary Biochemistry, College of Veterinary Medicine, Seoul National University, Seoul 08826, Republic of Korea
[e] KU Leuven, Department of Cellular and Molecular Medicine, Leuven 3000, Belgium
[f] Department of Agricultural Biotechnology, Seoul National University, Seoul 08826, Republic of Korea
[g] Department of Cardiovascular Biology and Medicine, Niigata University Graduate School of Medical and Dental Sciences, Niigata 951-8510, Japan
[h] Division of Cardiology, Department of Internal Medicine, College of Medicine Kosin, University Busan, Republic of Korea
[i] School of Biotechnology and Biomedical Science, Inje University, Kimhae 50834, Republic of Korea

ARTICLE INFO

Keywords:
Tetrahydrobiopterin
Proteomics
Mitochondrial biogenesis
PGC1α
Cardiovascular metabolism

ABSTRACT

Tetrahydrobiopterin (BH4) shows therapeutic potential as an endogenous target in cardiovascular diseases. Although it is involved in cardiovascular metabolism and mitochondrial biology, its mechanisms of action are unclear. We investigated how BH4 regulates cardiovascular metabolism using an unbiased multiple proteomics approach with a sepiapterin reductase knock-out ($Spr^{-/-}$) mouse as a model of BH4 deficiency. $Spr^{-/-}$ mice exhibited a shortened life span, cardiac contractile dysfunction, and morphological changes. Multiple proteomics and systems-based data-integrative analyses showed that BH4 deficiency altered cardiac mitochondrial oxidative phosphorylation. Along with decreased transcription of major mitochondrial biogenesis regulatory genes, including *Ppargc1a*, *Ppara*, *Esrra*, and *Tfam*, $Spr^{-/-}$ mice exhibited lower mitochondrial mass and severe oxidative phosphorylation defects. Exogenous BH4 supplementation, but not nitric oxide supplementation or inhibition, rescued these cardiac and mitochondrial defects. BH4 supplementation also recovered mRNA and protein levels of PGC1α and its target proteins involved in mitochondrial biogenesis (mtTFA and ERRα), antioxidation (Prx3 and SOD2), and fatty acid utilization (CD36 and CPTI-M) in $Spr^{-/-}$ hearts. These results indicate that BH4-activated transcription of PGC1α regulates cardiac energy metabolism independently of nitric oxide and suggests that BH4 has therapeutic potential for cardiovascular diseases involving mitochondrial dysfunction.

1. Introduction

Heart failure is a major cause of death and recurrent hospitalization. Despite the use of several therapies, including pharmacological antagonists such as angiotensin-converting enzyme inhibitors, angiotensin receptor blockers, and β-blockers and implantation of devices such as pacemakers and defibrillators, the 5-year mortality rate is still around 50% [1]. As heart failure is closely related to increased oxidative stress and mitochondrial dysfunction, restoring mitochondrial function has emerged as a promising therapeutic strategy [2]. Recently, the Q-SYMBIO trial showed that mitochondria-targeting coenzyme Q10 treatment improves the survival rate of chronic heart failure patients.

Abbreviations: BH4, tetrahydrobiopterin; EF, ejection fraction; eNOS, endothelial nitric oxide synthase; i.p., intraperitoneal; LV, left ventricle; NO, nitric oxide; NOS, nitric oxide synthase; OXPHOS, oxidative phosphorylation; ROS, reactive oxygen species

* Corresponding authors.
** Correspondence to: J. Han, College of Medicine, Cardiovascular and Metabolic Disease Center, Inje University, Busan 47392, Republic of Korea.
E-mail addresses: mbyspark@inje.ac.kr (Y.S. Park), sukim@postech.ac.kr (S. Kim), phyhanj@inje.ac.kr (J. Han).
[1] These authors contributed equally to this work.

https://doi.org/10.1016/j.bbadis.2019.07.018
Received 26 March 2019; Received in revised form 10 July 2019; Accepted 29 July 2019
Available online 03 August 2019

Although this trial has clinical limitations, it demonstrates the potential of mitochondria-targeting therapy [3].

Tetrahydrobiopterin (BH4) is a multifunctional cofactor implicated in the regulation of nervous, immune, and cardiovascular systems that acts as a combined enzymatic cofactor, nitric oxide synthesis (NOS) cofactor, and scavenger of reactive oxygen species (ROS) [4]. However, BH4 is also susceptible to oxidation and is reduced by high levels of oxidative stress [4]. Low levels of BH4 are associated with a broad range of cardiovascular diseases including hypertension, hypertrophy, and ischemic heart disease in animal models and human patients [4,5]. We previously demonstrated that BH4 deficiency increases ROS generation and mitochondrial dysfunction independent of nitrogen oxide (NO) in the amoeba system, whereas BH4 treatment reverses these abnormalities [6]. Although existing evidence suggests a link between BH4 and regulation of mitochondrial function [7], little is known about the effects of BH4 on mitochondria-mediated heart energy metabolism. Therefore, it is important to determine whether BH4 plays a role in cardiac function and mitochondrial energy metabolism and elucidate the underlying mechanisms.

Sepiapterin reductase (SPR) is a rate-limiting enzyme that catalyzes the final step of BH4 biosynthesis. We previously found that *Spr*$^{-/-}$ mice exhibit BH4 deficiency in the liver and brain, dwarfism, and impaired body movements and are suitable for studying the physiological and clinical consequences of BH4 deficiency [8]. However, no studies have examined cardiac and mitochondria function using this mouse model.

As systemic proteomic analysis is an unbiased approach to identifying novel biological mechanisms, we performed systems-based integrative data analysis to investigate systematic changes in the cardiac mitochondrial proteome of *Spr*$^{-/-}$ mice and organized identified proteins into specific cardiovascular metabolic pathways affected by BH4 deficiency. We demonstrated that BH4 is required for proper mitochondrial function, energy provision, ROS regulation, and contractile function in cardiac muscle using *Spr*$^{-/-}$ mice. We further demonstrated that BH4 enhances PGC1α transcription and stimulates cardiovascular energy metabolism signaling pathways.

2. Methods

2.1. Experimental animals and drug treatment

Animal studies conformed to the Guide for the Care and Use of Laboratory Animals published by the US National Institutes of Health (NIH Publication No. 85-23, revised 1996) and was approved by the Inje Medical University Institutional Animal Care and Use Committee (approval number 2011-049).

Five-week-old male *Spr*$^{-/-}$ mice and same-aged male C57BL/6J wild-type (WT) controls were used to study the mechanism of BH4 deficiency [8]. Five-week-old male eNOS knock-out (KO) mice were provided by Dr. Goo Taeg Oh (Ewha Women's University, Seoul, Republic of Korea). All mice were kept in a specific pathogen-free facility with controlled temperature (20–24 °C) and humidity (40–70%), a 12-h light cycle, and free access to standard laboratory chow and tap water.

For the functional rescue and survival study, three-week-old *Spr*$^{-/-}$ mice were treated for up to 4 weeks with intraperitoneal (i.p.) bolus injections of 100 μl vehicle (normal saline), BH4 (20 mg/kg/day; Cayman Chemical, Ann Arbor, MI), or diethylenetriamine NONOate (0.4 mg/kg/day; Cayman Chemical) as a source of NO. The NOS inhibitor nitro-L-arginine methyl ester hydrochloride (L-NAME, Sigma-Aldrich, 50 mg/kg/day i.p. bolus injection) was co-administered with BH4 to exclude NO-dependent effects of BH4.

2.2. H&E staining and electron microscopy

To assess changes in cardiac tissue histology, hematoxylin and eosin (H&E) staining was performed on formalin-fixed cardiac tissue from WT and *Spr*$^{-/-}$ mice. Isolated heart tissue was fixed in 10% polyformaldehyde, embedded in paraffin wax, and cut into 4-μm sections that were stained with H&E. Stained sections were characterized morphologically under an optical microscope at 500× magnification. Transmission electron microscopy was used to detect morphological differences between WT and *Spr*$^{-/-}$ mouse cardiac mitochondria [9].

2.3. Measurement of cardiac BH4 concentration

Cardiac tissue was homogenized in 5 μl/mg extraction buffer containing 50 mM Tris-HCl (pH 7.5), 1 mM EDTA, 0.1 M KCl, 1 mM DTT, and 0.2 mM phenylmethylsulfonyl fluoride. Homogenates were centrifuged at 12,000*g* for 20 min at 4 °C. Supernatants were subjected to differential oxidation in acidic (0.4 mol/l trichloroacetic acid) or alkaline (0.4 mol/l NaOH) solutions containing 1% I2/2% KI in 0.2 M tricarboxylic acid (TCA) or 1% I2/2% KI in 0.2 M NaOH for 1 h in the dark. After centrifugation, 20 μl supernatant was injected into a high-performance liquid chromatography (HPLC) system with a fluorescence detector. Excitation and emission wavelengths of 350 and 450 nm, respectively, were used to detect fluorescent BH4 and its oxidized species.

2.4. Measurement of cardiac Spr activity

Reactions were performed in phosphate buffer (0.1 mol/l, pH 7.5) containing a final concentration of 0.1 mmol/l sepiapterin, 0.2 mmol/l NADPH, and 5 μg cardiac tissue lysate. Enzymatic reactions were conducted at 37 °C for 2 h in the dark, and the biopterin conversion rate was used as an index of *Spr* activity. The reaction was stopped by incubation in 10 μl iodine solution containing 2% K/1% I2 in 1 M HCL for 10 min in the dark. Precipitated proteins were removed by centrifugation at 13,000*g* for 10 min at room temperature. Excess iodine was quenched by adding 25 μl 2% ascorbic acid. The resulting biopterin content was measured with an HPLC system (Waters Spherisorb 5 ODS-1 column, Gilson 321 model). Fluorescence was monitored with an HP 1046 fluorescent detector at 350 nm excitation and 450 nm emission wavelengths. Flow rate was maintained at 1.2 ml/min. The chromatographic profile was analyzed using EZstart chromatography software (Shimadzu).

2.5. Echocardiography measurement

Echocardiographic measurement with the high-resolution echocardiograph system Vivid 7 (GE Healthcare) was used to detect cardiac structure alterations and cardiac function in vivo using an i13L-15MHz probe. We obtained measurements of M-mode intraventricular septum (IVS), left ventricular internal diameter (LVID), left ventricular posterior wall (LVPW), end diastolic volume (EDV), end systolic volume (ESV), stroke volume (SV), ejection fraction (EF), and fractional shortening (FS) in conscious mice. All data and images were saved and analyzed on an EchoPAC PC (GE Healthcare).

2.6. Isolation and purification of myocardial mitochondria

After sacrifice, mouse hearts were rapidly removed, washed, and homogenized using a medium fitting glass-Teflon Potter-Elvehjem homogenizer in ice-cold mitochondrial isolation buffer (MIB) containing 50 mM sucrose, 200 mM mannitol, 5 mM potassium phosphate, 1 mM EGTA, 5 mM MOPS, 0.1% BSA (w/v), and a protease inhibitor cocktail, and pH was adjusted to 7.4. The resulting homogenate was centrifuged at 1000*g* for 10 min at 4 °C to remove nuclei and cell debris. The supernatant was centrifuged at 10,000*g* for 10 min at 4 °C to precipitate mitochondria, which were washed with 5 ml ice-cold MIB and centrifuged again at 10,000*g* for 10 min at 4 °C. Isolated mitochondria were used for mitochondrial functional analysis including oxygen consumption, adenosine triphosphate (ATP) production assay, complex activity assays, and ROS production assay. For mitochondria proteomic

analysis, isolated mitochondria pellets were further purified by gentle homogenization in 5 ml 19% Percoll in MIB for purification on a Percoll density gradient. This gradient was prepared by careful stepwise layering of 3 ml 52%, 3 ml 42%, and 3 ml 31% Percoll solutions in a centrifuge tube. Crude mitochondrial fractions (containing 19% Percoll) were layered on top of the Percoll density gradient and centrifuged at 100,000*g* for 1 h at 4 °C. The major band at the interface of the 52% and 42% Percoll solutions was collected, diluted with three volumes of MIB, and centrifuged twice at 15,000*g* for 10 min [10].

2.7. Permeabilization of cardiac fiber

Permeabilization of cardiac fiber was performed as previously described [11]. Briefly, the left ventricles of isolated hearts were dissected to 10–25 mg wet weight tissue. Dissected tissue was further mechanically separated into a final 1–3 mg wet weight fiber bundle by sharp forceps. The fiber bundle was incubated in preservation solution (2.77 mM CaK_2EGTA, 7.23 mM K_2EGTA, 20 mM imidazole, 0.5 mM dithiothreitol, 20 mM taurine, 50 mM K-MES, 6.56 $MgCl_2$, 5.7 mM ATP, 14.3 mM phosphocreatine, pH 7.1) with 50 μg/ml saponin for 20 min on ice. The fiber bundle was rinsed three times with MiR05 buffer (0.5 mM EGTA, 3 mM $MgCl_2.6H_2O$, 20 mM taurine, 10 mM KH_2PO_4, 20 mM HEPES, 1 g/l BSA, 60 mM potassium-lactobionate, 110 mM sucrose, pH 7.1, adjusted at 30 °C). Permeabilized fiber (1–3 mg) was used for in situ oxygen consumption measurement.

2.8. Proteome analysis

Two-dimensional gel electrophoresis mass spectrometry (2DE-MS) [12] and one-dimensional liquid chromatography tandem mass spectrometry (LC-MS/MS) proteome analysis [13] were performed to identify differentially expressed proteins (DEPs) in the cardiac mitochondria of WT and $Spr^{-/-}$ mice.

2.9. Quantification of protein abundance and identification of remodeled metabolic pathways

To estimate the abundance of *mt* proteins isolated from three $Spr^{-/-}$ and two WT mouse hearts, we employed label-free quantitative proteomic analysis using the differential absolute protein expression measurement (APEX) technique [14]. The relative protein abundance ratio was calculated by dividing *mt* protein abundance in $Spr^{-/-}$ mice by that in WT mice. Quantified *mt* proteome sets were validated through systems-based data-integrative analysis.

To identify remodeled pathways in $Spr^{-/-}$ mice, we mapped our quantified *mt* proteins onto biological pathways compiled from the Kyoto Encyclopedia of Genes and Genomes (KEGG) database [15]. We calculated an enrichment value [$E(M_i)$] to measure the existence of DEPs in a given pathway as an indicator of pathway remodeling. We randomly permutated the existence of proteins 10,000 times to obtain a null $E(M_i)$ distribution for each pathway map (M_i) and assumed Gaussian distributions. A pathway was considered to be remodeled if its *p*-value was < 0.01.

2.10. In vitro SPR knock-down

Lentiviral transduction particles containing mouse *SPR* shRNA was purchased from Sigma-Aldrich (SHCLNV-NM_011467). HL-1 cells, a cardiomyocyte cell line, were kindly provided by Dr. William Claycomb (Louisiana State University Health Science Center, New Orleans, LA) and were cultured as previously described [16]. To generate cell lines with stable knock-down of *SPR*, HL-1 cells, (2×10^5 cells in a 6-well plate) were infected with shRNA lentiviral transduction particles and hexadimethrine bromide at a final concentration of 8 μg/ml. Cells were incubated for 4 h, after which the medium containing lentiviral particles was removed. After 24 h, infected cells were selected by culture in the presence of puromycin (1 μg/ml). Selected clones were maintained in medium containing puromycin (0.1 μg/ml).

2.11. Mitochondrial function analysis

To estimate mitochondria functional integrity, we compared ΔΨm between WT and $Spr^{-/-}$ mice using the mitochondrial membrane-specific fluorescent probe tetramethylrhodamine ethyl ester perchlorate (TMRE) [9]. Mitochondrial oxygen consumption was determined using an Oxygraph 2-k (Oroboros Instrument, Innsbruck, Austria) [11]. Complex I, II, III, and IV activities were measured in frozen isolated mitochondrial hearts using a 96-well plate-based assay. Complex I, II, and IV activities were determined using the Complex I, II, and IV Enzyme Activity Microplate Assay Kit (MitoSciences. OR. USA) following the manufacturer's recommended protocol and settings. Complex III activity was determined using a modified MitoTOX™ OXPHOS Complex III Activity Kit (MitoSciences). Data are presented as mOD/min [17]. ATP concentration was measured in cardiac tissue homogenates as previously described [9]. Mitochondrial ROS production was assessed in isolated mitochondria using specific fluorescence probes and flow cytometry [18].

2.12. Statistical analysis

All results are expressed as mean ± standard error of the mean (SEM). Differences between two groups were analyzed using unpaired, two-tailed Student's *t*-tests. Differences between more than two groups were analyzed using one-way analysis of variance (ANOVA) followed by Bonferroni post hoc tests. In all analyses, $p < 0.05$ was considered statistically significant. All analyses were performed using Origin 8.0 (OriginLab, Northampton, MA, USA).

*An expanded Experimental Procedures is available in the online Supplementary information.

3. Results

3.1. Cardiac damage and contractile dysfunction induced by BH4 deficiency

Compared with WT mice, $Spr^{-/-}$ mice showed significant growth retardation (Fig. 1A), reduced physical activity (Movie S1), reduced SPR activity (Fig. 1B), reduced cardiac BH4 concentration (Fig. 1C), and a markedly shortened life span (Fig. 1D).

BH4 deficiency modified cardiac morphology and contractility. Heart and muscle fiber size were significantly decreased in $Spr^{-/-}$ mice (Fig. 1Ea–d and F), with muscle fiber degeneration and lymphocytic infiltration observed in $Spr^{-/-}$ cardiac muscle (Fig. 1Ee–f). Markers of tissue damage and heart failure (i.e., lactate dehydrogenase level and *Nppa* and *Nppb* expression) [19] were elevated in $Spr^{-/-}$ mice (Fig. 1G and H). $Spr^{-/-}$ mice had impaired cardiac contractility (Fig. 1I–K). Specifically, assessment of left ventricular (LV) geometry showed decreased systolic indices, including reduced IVSs and increased LVIDs (Fig. 1I). Due to contractile dysfunction, ESV was increased and SV was decreased (Fig. 1J) in $Spr^{-/-}$ hearts. $Spr^{-/-}$ hearts also showed abnormal LV systolic functional parameters, including decreased EF and FS rate (Fig. 1K). These results indicate that BH4 deficiency induces severe LV systolic dysfunction.

3.2. Systems analysis of differentially expressed mitochondrial proteins in $Spr^{-/-}$ mice

Phenotypic alterations are associated with changes in protein expression [20]. To characterize differences in protein expression levels between WT and $Spr^{-/-}$ mitochondria, we used quantitative multiple proteomic analysis to compare abundances of *mt* proteins. Mitochondrial proteins obtained from heart tissue of $Spr^{-/-}$ and WT mice were

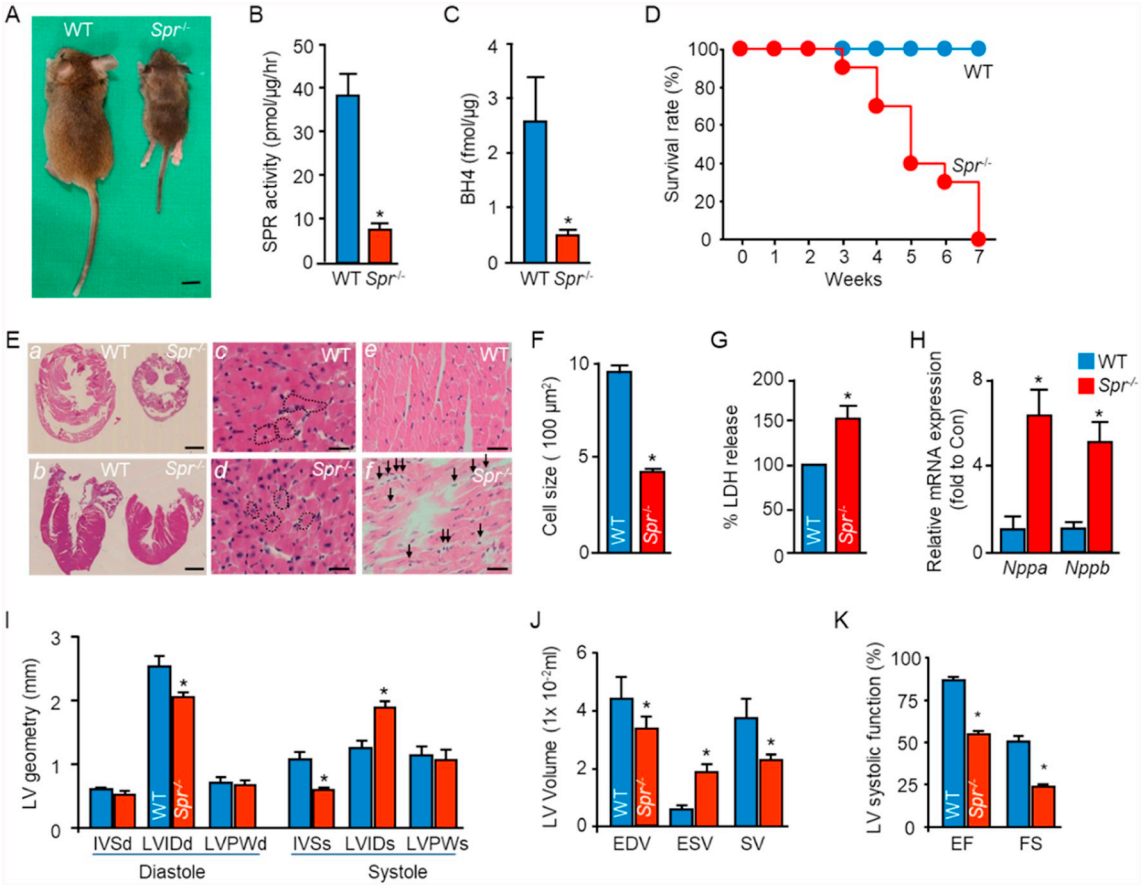

Fig. 1. Altered cardiac tissue morphology and contractility in *Spr*$^{-/-}$ mice. (A) Phenotypic characterization of *Spr*$^{-/-}$ and WT mice (scale bar: 1 cm). (B) SPR activity in the heart. (C) BH4 concentration in the heart. (D) Survival rate. (E) Cross-sectional (a) and longitudinal (b) H&E-stained heart sections (scale bar: 1 mm) and cardiac muscle fiber (c, d; scale bar: 25 μm). Cross-sectional muscle fiber with lymphocytic infiltration (e, f; scale bar: 25 μm). (F) Cross-sectional myocyte size quantification. (G) Relative blood lactate dehydrogenase (LDH) level. (H) *Nppa* and *Nppb* expression. (I) LV geometry of WT and *Spr*$^{-/-}$ mice during systole (s) and diastole (d). (J) LV volume during systole and diastole. (K) Cardiac systolic function of WT and *Spr*$^{-/-}$ mice. (A–C) and (E–K), $n = 5$; (D), $n = 7$. *$p < 0.05$ vs. WT, two-tailed Student's *t*-tests. (See also online Movie S1.)

identified using 2DE-MS and LC-MS/MS analysis. 2DE-MS identified 30 mitochondrial DEPs, which were mainly related to the oxidative phosphorylation system (OXPHOS; Fig. 2Aa), fatty acid metabolism (Fig. 2Ab), amino acid metabolism (Fig. 2Ac), carbohydrate metabolism (Fig. 2Ad), post-translational modifications (Fig. 2Ae), and the cytoskeleton (Fig. 2Af) (Supplementary Table S1).

To enhance the accuracy, reliability, and coverage of proteomics analyses, we performed parallel LC-MS/MS proteomics. We matched, on average, 4908 LC-MS/MS peptide spectra to 204 proteins with a 95% confidence level (Supplementary Table S2). Our approach to measuring protein abundance and identifying reliable mitochondrial proteins is depicted in Fig. 2B. To measure protein abundance, we employed label-free quantitative proteomic analysis based on the observation that the number of LC-MS/MS spectra is associated with the abundance of the corresponding protein [21]. For the spectral counting approach, protein abundance was estimated by dividing the number of LC-MS/MS spectra from all peptides corresponding to a given protein by the number of all LC-MS/MS spectra for all proteins in the experiment (see Methods and Supplementary information). The estimated protein abundances of the proteome sets had excellent reproducibility (Fig. 2C). Pairwise comparisons of the three *Spr*$^{-/-}$ *mt* proteome sets showed an average Pearson's correlation coefficient of 0.86 (Fig. 2C, dark blue), whereas those between the two WT *mt* proteome sets averaged 0.90 (Fig. 2C, light blue). We measured the abundance ratios of 176 proteins by comparing *Spr*$^{-/-}$ and WT *mt* proteome sets (Supplementary Table S3). The protein abundance ratio was defined as the median of six abundance ratios (see Supplementary information). We confirmed the reliability of the protein abundance ratio through comparisons between independent 2DE-MS and LC-MS/MS analyses. Twenty of the 30 proteins identified in the 2DE-MS analysis matched those obtained from the label-free quantitative proteomic analysis (Fig. 2D).

Next, we used a systems-based data-integrative approach to evaluate our proteome set. Because data from proteomic analysis only provide isolated protein information, presumably with some false positives [22], we used a data-integrative approach to identify reliable *mt* proteins. We compared our proteome set with previously characterized *mt* proteome sets from mouse hearts [23,24] and confirmed that 98% (172 of 176) proteins matched known *mt* proteins (Fig. 2E, Supplementary Table S4). We investigated the physical and/or functional associations of these 172 proteins based on the notion that protein pairs that physically interact or share similar functions tend to be located in the same subcellular organelle [25]. We identified 164 reliable *mt* proteins that were physically and/or functionally associated with each other (Supplementary Table S5). To select DEPs, we examined the fraction of proteins according to protein abundance ratios. The expression levels of 55 proteins changed > 1.5-fold in *Spr*$^{-/-}$ mice and were thus defined as DEPs (Fig. 2F), whereas the remaining proteins were classified as non-differentially expressed proteins (NEPs).

3.3. Remodeled mitochondrial metabolic pathways in *Spr*$^{-/-}$ mice

Proteins rarely act alone but rather interact with other proteins and comprise specific pathways responsible for various biological processes

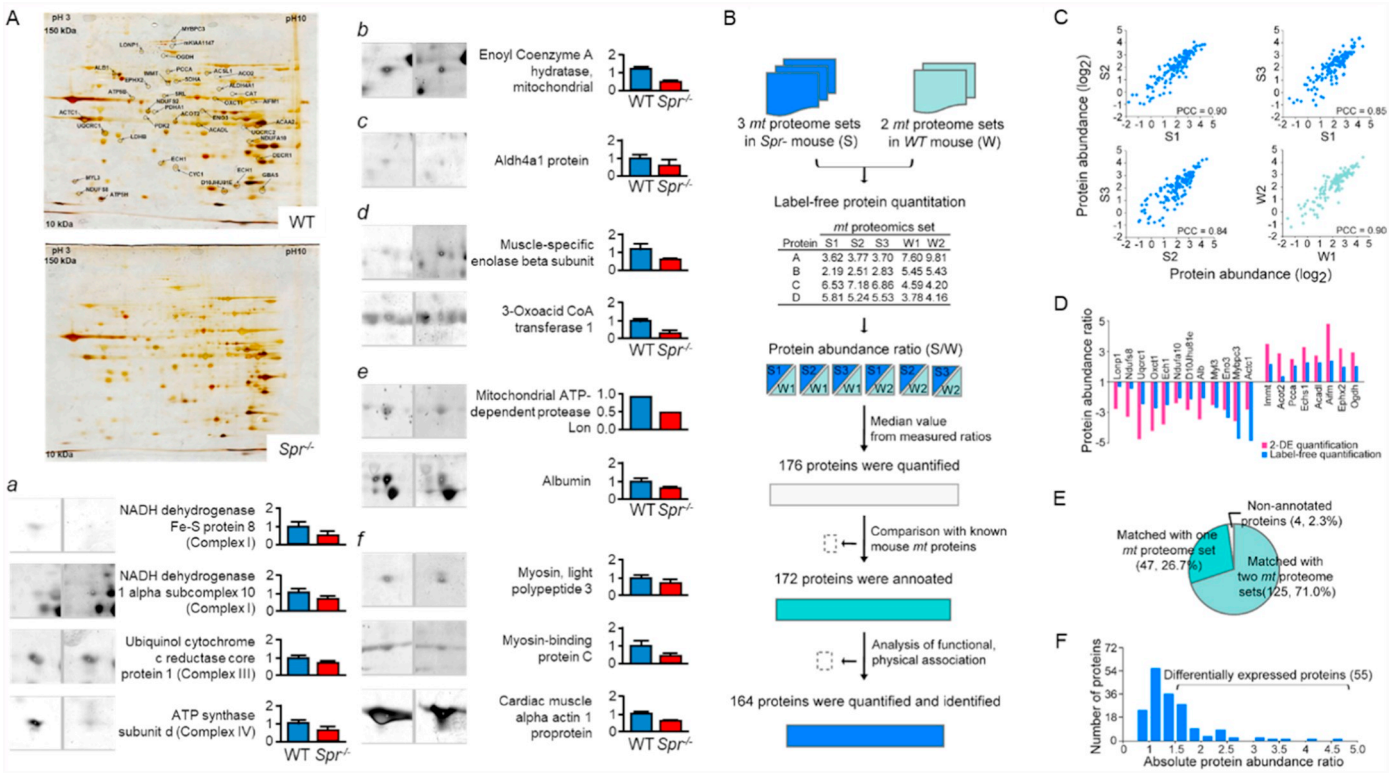

Fig. 2. Multi-proteomics approach to identify cardiac mitochondrial DEPs in *Spr*$^{-/-}$ mice. (A) Silver-stained 2DE gels from WT (top) and *Spr*$^{-/-}$ (bottom) mice. Enlarged images of significantly reduced proteins in *Spr*$^{-/-}$ compared with WT mice and their biological categories according to the Clusters of Orthologous Groups of proteins algorithm: oxidative phosphorylation (a), fatty acid metabolism (b), amino acid metabolism (c), carbohydrate metabolism (d), post-translational modifications and chaperones (e), and cytoskeleton (f). (B) Flow diagram of procedure to measure protein abundance and reliably identify mitochondrial proteins. (C) Reproducibility of protein abundance. Comparison of mitochondrial proteomic sets between *Spr*$^{-/-}$ (dark blue) and WT (light blue) mice. (D) Similar expression patterns were observed using label-free quantitation (red) and 2DE analysis (blue). (E) Relative contributions of other mouse heart mitochondrial proteomic sets. (F) Distribution of protein abundance ratios.

[26]. These associations are of particular importance for relating genotype to phenotype at the molecular level. Moreover, alterations in expression could induce remodeling of specific metabolic pathways, leading to phenotypic differences between WT and *Spr*$^{-/-}$ mice. To identify remodeled metabolic pathways related to differentially expressed *mt* proteins, we constructed a protein-pathway network (Fig. 3A and Supplementary Table S5), a bipartite network composed of two different types of nodes. One set was our *mt* proteome set, and the other consisted of metabolic pathways compiled from the KEGG database [15]. A protein and pathway are linked if the protein acts as a metabolite or substrate in the pathway. In the resulting protein-pathway network, 13 *mt* metabolic pathways appeared to be remodeled in *Spr*$^{-/-}$ mice (red triangles in Fig. 3A). These remodeled pathways were connected by 102 *mt* proteins, including 37 DEPs (dark blue circles) and 65 NEPs (light blue circles).

We also identified two biologically relevant unipartite networks from the bipartite protein-pathway network that contained a pathway-pathway network (Fig. 3B) and a protein-protein network (Fig. 3C). In the pathway-pathway network (Fig. 3B), nodes indicate pathways, and two pathways are connected if they share at least one protein. We found that 12 of 13 identified pathways were interconnected and formed a major network, indicating that the phenotypic alterations of *Spr*$^{-/-}$ mice arose from the close associations of *mt* metabolic pathways. These 12 pathways were divided into four groups based on their biological functions: energy production, lipid metabolism, carbohydrate metabolism, and amino acid metabolism (Supplementary Table S6).

The resulting protein-protein network (Fig. 3B) consisted of 102 *mt* proteins with 1541 interactions in which the number of interactions per single protein varied from 3 to 61 depending on the specific pathway. The OXPHOS pathway had the highest number of interactions among the 13 remodeled pathways (Fig. 3C), with proteins interacting twice as much as in other pathways (i.e., the 45 proteins in the OXPHOS pathway had an average 44.76 interactions). This suggests that expression changes in OXPHOS complexes may have a major impact on pathway remodeling in abnormal *Spr*$^{-/-}$ mitochondria.

We identified six significantly remodeled pathways in *Spr*$^{-/-}$ mitochondria by measuring the enrichment of DEPs in specific pathways (Table 1; corresponding to *p*-values for DEP enrichment < 0.01): the OXPHOS pathway (KEGG:mmu00190), branched-chain amino acid metabolism (mmu00280), TCA cycle (mmu00020), glycolysis (mmu00010), fatty acid metabolism (mmu00071), and pyruvate metabolism (mmu00620). The KEGG biological pathway "mmu00010: glycolysis/gluconeogenesis" category includes mitochondrial and non-mitochondrial compartment proteins, with 16 proteins related to glycolysis mainly located in "mitochondria" or "mitochondria and cytoplasm."

All pathways were interconnected by 36 DEPs (Fig. 3D). The OXPHOS pathway appeared to be the most remodeled, with 33.3% of all DEPs (12 of 36 DEPs) and around twice as many DEPs as in the other identified pathways (Table 1). In addition, six DEPs were located at complex I (Fig. 3E), suggesting that this complex is a primary target and/or source of environmental and endogenous oxidative stress causing mitochondrial dysfunction [27].

3.4. Altered mitochondrial morphology and oxidative phosphorylation induced by BH4 deficiency

To determine the consequences of metabolic pathway remodeling due to BH4 deficiency, we analyzed several aspects of the mitochondrial biogenesis and OXPHOS pathways. Nuclear and mitochondrial

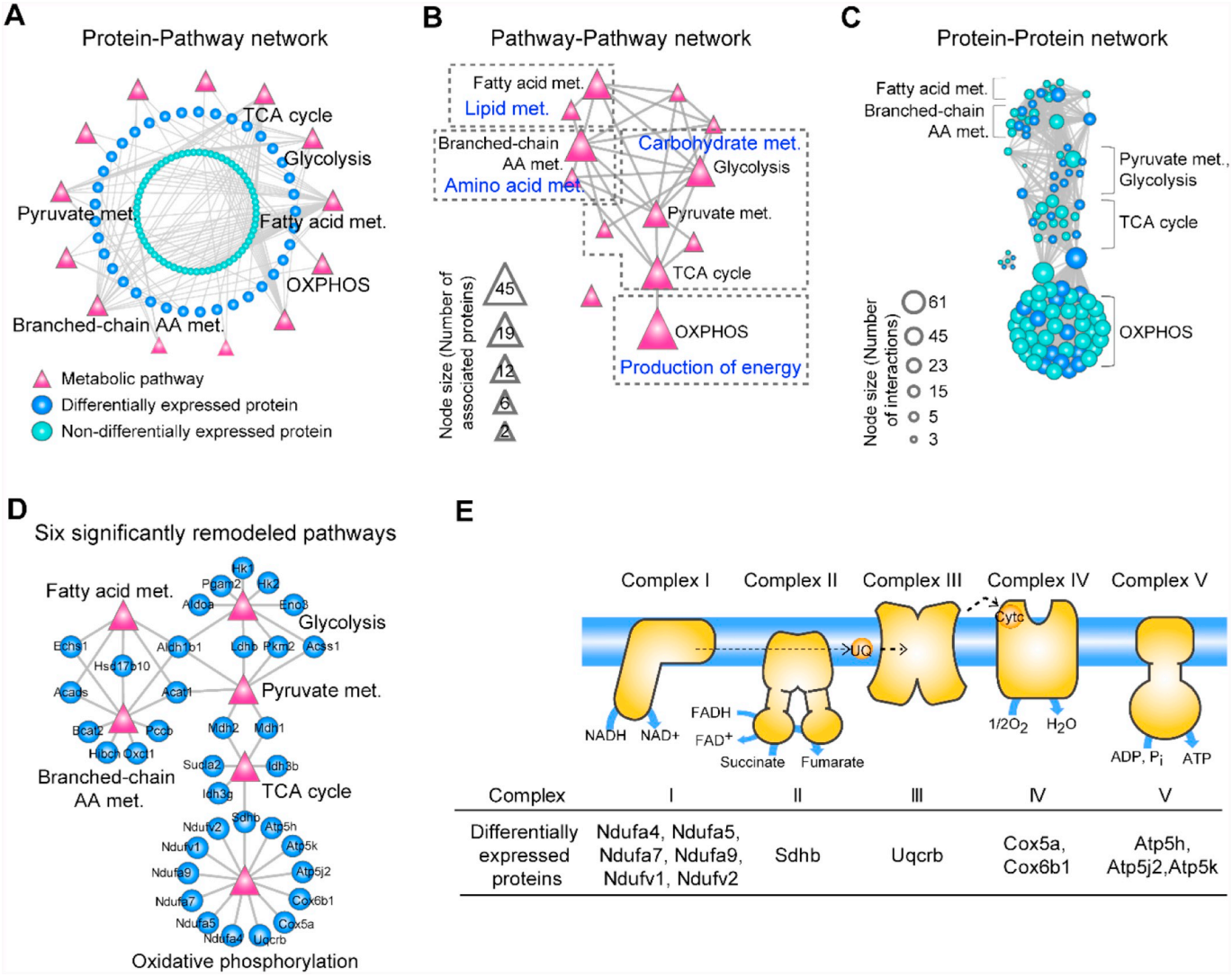

Fig. 3. Remodeled mitochondrial metabolic pathways in *Spr*$^{-/-}$ mice. (A) Protein-pathway network of mitochondria (*mt*). Nodes represent *mt* proteome set (circles) and *mt* metabolic pathways (red triangles). DEPs and NEPs are colored dark blue and light blue, respectively. Significantly remodeled pathways are labeled. (B) Pathway-pathway mitochondrial network. Node size represents the number of associated proteins. (C) Protein-protein mitochondrial network. Node size corresponds to the number of proteins sharing the same pathway. (D) Six significantly remodeled pathways in *Spr*$^{-/-}$ mice shown as red triangles. (E) The maximally remodeled OXPHOS pathway. DEPs involved in five OXPHOS complexes are tabulated.

transcriptional regulators tightly modulate mitochondrial biogenesis, transcription of mtDNA, and translation of mRNA. We evaluated mRNA expression levels of important regulators of mitochondrial biogenesis (*Ppargc1a*, *Ppara*, and *Esrra*), modulators of mtDNA transcription and mRNA translation (*Tfam*, *Tfb1m*, *Tfb2m*, *Ssbp1*, *Polrmt*, and *Tufm*), regulators of mitochondrial protein import and stabilization (*Phb1*, *Phb2*, and *Immt*), and a mtDNA quantitative marker (*mt-Cytb*) (Fig. 4A). BH4 deficiency reduced gene expression of all regulators of mitochondrial biogenesis and three modulators of mtDNA transcription and mRNA translation (*Tfam*, *Ssbp1*, and *Polrmt*).

Consistent with the transcriptional deficiency of several genes regulating the biogenesis of mitochondria, *Spr*$^{-/-}$ mice had fewer cardiac mitochondria and altered intra-mitochondrial structure. Compared with the dark, dense, intact mitochondria in control tissue (Fig. 4Ba–b), mitochondria in *Spr*$^{-/-}$ cardiac tissue had pale matrices and shortened, disorganized cristae displaced to the periphery (Fig. 4Bc–d) in electron microscopic images. The number and total volume of cardiac mitochondria in *Spr*$^{-/-}$ mice were decreased to approximately 60% and 53%, respectively, of WT values (Fig. 4B–C). *Spr*$^{-/-}$ hearts showed higher proportions of abnormal mitochondria showing disrupted cristae

Table 1
Significantly remodeled pathways in *Spr*$^{-/-}$ mitochondria.

Pathway	KEGG ID	Number of identified proteins	Number of DEPs	DEP enrichment (*p*-value)
Oxidative phosphorylation	190	45	12	3.53E−09
Branched-chain amino acid metabolism	280	19	7	2.86E−09
TCA cycle	20	19	4	3.77E−04
Glycolysis	10	16	8	5.53E−21
Fatty acid metabolism	71	15	4	9.95E−05
Pyruvate metabolism	620	12	4	6.26E−06

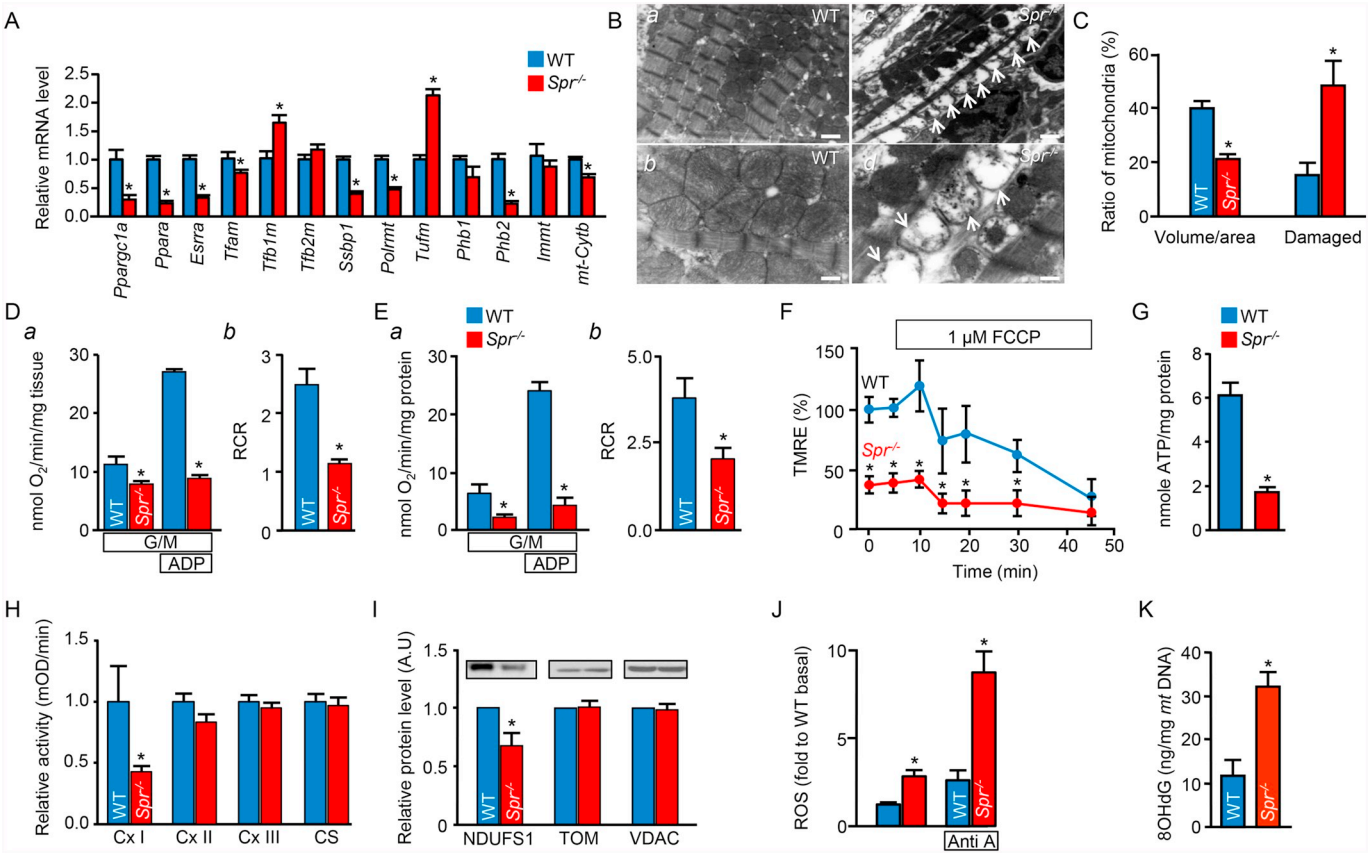

Fig. 4. Impaired mitochodrial biogenesis and oxidative phosphorylation induced by BH4 deficiency. (A) Real-time PCR results of major mitochondrial biogenesis regulatory genes. (B) Representative electron micrographs of cardiac tissue from WT (n = 3; a, b) and *Spr*$^{-/-}$ (n = 3; c, d) mice at different magnifications (a, c: 6000×; b, d: 15,000×). Scale bars, a and c: 1 μm; b and d: 0.5 μm. Arrows indicate mitochondria with pale matrices and shortened, disorganized cristae displaced to the periphery. (C) Mitochondrial volume in cross-sectional cardiac tissue (left) and proportion of abnormal mitochondria (right). n = 3 mice/group; 5 images/mouse; *p < 0.05 vs. WT. (D) Mitochondrial OCR in permeabilized cardiac tissue. Respiration rates with glutamate and malate (G/M; state 4) and glutamate, malate, and ADP (state 3) (left) and RCR (state4/state3) (right). (E) OCR in isolated mitochondria. Respiration rates with glutamate, malate, and ADP (left) and RCR (right). (F) Basal levels of mitochondrial membrane potential (ΔΨm) and FCCP-induced depolarization in TMRE-stained isolated cardiac mitochondria. (G) ATP concentration in cardiac tissue. (H) Oxidative phosphorylation complex (Cx) I, II, and III and citrate synthase (CS) activity in isolated cardiac mitochondria. (I) NDUFS1 in isolated cardiac mitochondria. Translocase of the outer membrane (TOM) and voltage-dependent anion channel (VDAC) served as internal controls. a.u., arbitrary units. (J) Baseline and antimycin A (Anti A)-induced mitochondrial ROS production levels. (K) Oxidative mtDNA damage. n = 5 mice/group. *p < 0.05 vs. WT, two-tailed Student's t-tests (A, C, D, E, G, H, I, J, and K), two-way ANOVA followed by Bonferroni post hoc tests (F).

(Fig. 4C) and small fragmented mitochondria (< 0.1 μm^2; Supplementary Fig. 1).

We directly tested the proteomics-derived hypothesis that BH4 deficiency results in cardiac mitochondrial OXPHOS dysfunction. The oxygen consumption rate (OCR) in *Spr*$^{-/-}$ mice was significantly decreased in both permeabilized cardiac tissue (Fig. 4D) and isolated cardiac mitochondria (Fig. 4E). In the presence of 5 mM glutamate and malate (state 4 respiration), the OCR of *Spr*$^{-/-}$ mice was significantly reduced to 70% and 21% of WT cardiac tissue and isolated mitochondria, respectively. Additionally, the OCR of *Spr*$^{-/-}$ cardiac tissue and mitochondria in state 3 respiration (stimulated by adding 200 μM adenosine diphosphate [ADP]) was 35% and 18% of WT values, respectively. Consequently, the respiratory control ratio (RCR) was significantly decreased in *Spr*$^{-/-}$ cardiac tissue and mitochondria.

Mitochondrial membrane potential (ΔΨm) was significant depolarized in *Spr*$^{-/-}$ mice compared with WT mice as measured by fluorescence signal from the ΔΨm-specific probe tetramethylrhodamine ethyl ester (TMRE; Fig. 4F). The specificity of TMRE staining was verified using 1 μM carbonylcyanide-*p*-trifluoromethoxyphenylhydrazone (FCCP)-induced ΔΨm depolarization. Collectively, ΔΨm depolarization and the suppressed OCR were associated with reduced ATP production in *Spr*$^{-/-}$ mice (Fig. 4G). We also measured the activities of oxidative phosphorylation Complexes I, II, and III and citrate synthase to determine whether these complexes are primary targets of BH4 deficiency and found that *Spr*$^{-/-}$ mice exhibited significantly lower complex I activity (Fig. 4H). Western blot analysis revealed reduced expression of NADH dehydrogenase Fe—S protein 1 (NDUFS1) in an equal amount of isolated *Spr*$^{-/-}$ compared with WT mitochondria (Fig. 4I). These results further demonstrate the essential role of BH4 in mitochondrial energy metabolism in cardiac tissue.

BH4 deficiency also led to an imbalance in ROS dynamics. We measured mitochondrial ROS levels in the presence or absence of antimycin A, a specific inhibitor of mitochondrial complex III. Baseline mitochondrial ROS levels were 296% higher in *Spr*$^{-/-}$ mice than in WT mice, and antimycin A treatment increased ROS generation 3.7 times faster in *Spr*$^{-/-}$ mice than in WT mice (Fig. 4J). Furthermore, compared with WT mice, *Spr*$^{-/-}$ mice showed 2.75-fold higher levels of 8-hydroxydeoxyguanosine (8OhdG) released from damaged mtDNA (Fig. 4K).

3.5. Rescue of heart and mitochondrial abnormalities in *Spr*$^{-/-}$ mice by BH4 supplementation

To clarify whether mitochondrial dysfunction in *Spr*$^{-/-}$ mice is directly related to BH4 deficiency or is an indirect effect of *Spr* KO, we investigated the effect of BH4 supplementation in *Spr*$^{-/-}$ mice (*Spr*$^{-/}$

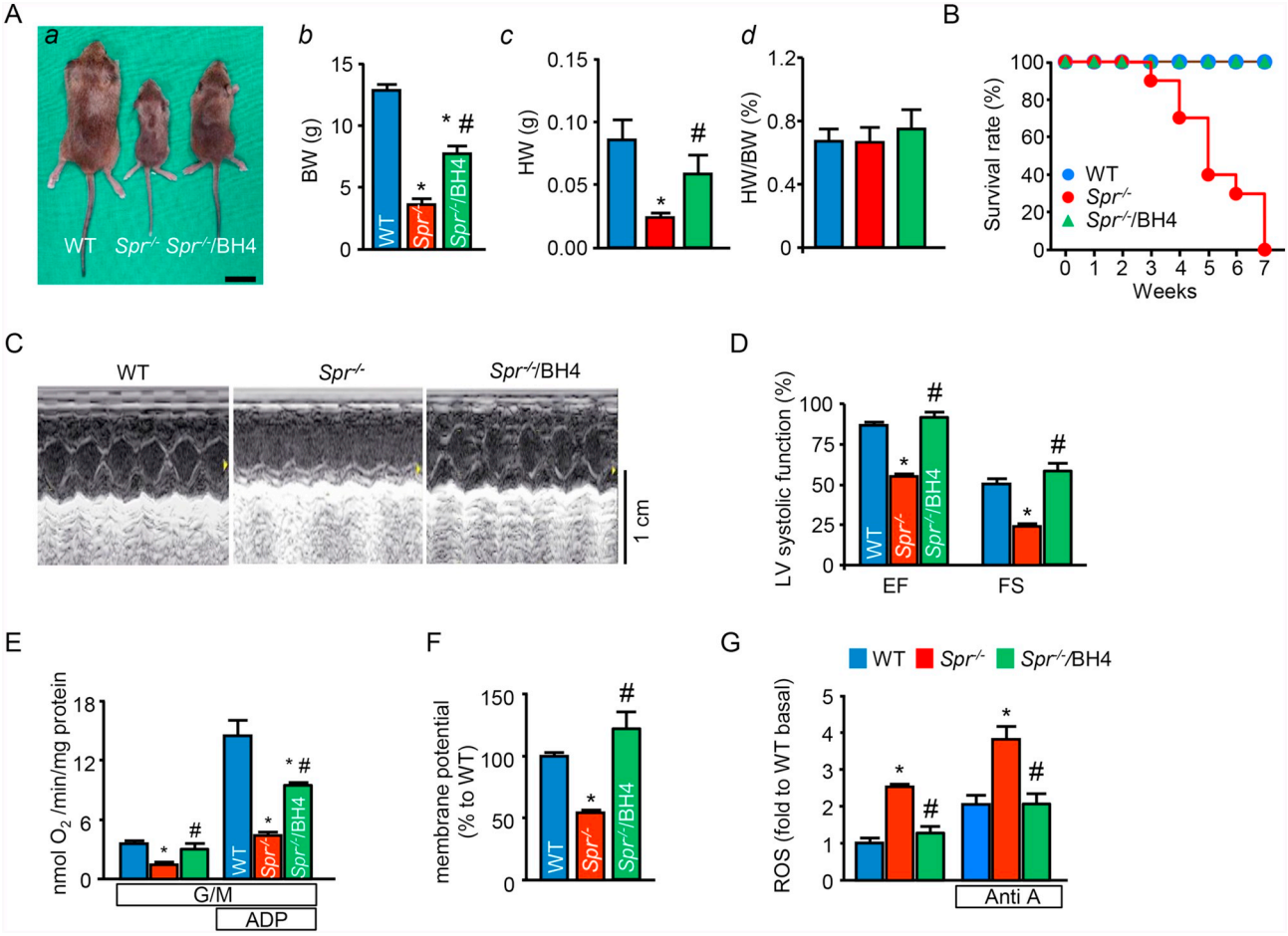

Fig. 5. Rescue of cardiac and mitochondrial dysfunction in $Spr^{-/-}$ mice by BH4 supplementation. (A) Phenotypic characterization (a, scale bar: 1 cm), body weight (BW, b), and heart weight (HW, c). (B) Survival rates. (C) Echocardiograms. (D) EF and FS. (E) Relative OCR. (F) Mitochondrial inner membrane potential. (G) Basal and antimycin A (Anti-A)-induced ROS level in isolated cardiac mitochondria. Data are expressed as mean ± SEM. *$p < 0.05$ vs. WT, #$p < 0.05$ vs. $Spr^{-/-}$, ANOVA with Bonferroni post hoc tests.

$^{-}$/BH4). Supplementation for 2 weeks with exogenous BH4 (20 mg/kg/day, i.p.) significantly increased the body size and weight of $Spr^{-/-}$ mice (Fig. 5A) and extended their life span (Fig. 5B). Cardiac systolic dysfunction recovered after BH4 supplementation (Fig. 5C–D). Suppression of mitochondrial OCR (Fig. 5E) and reduced ΔΨm (Fig. 5F) were significantly reversed in $Spr^{-/-}$/BH4 mice. BH4 supplementation also reduced ROS production (Fig. 5G).

BH4 couples with eNOS to produce NO. However, in the heart, unlike other tissues, eNOS is not involved in basal mitochondrial biogenesis [28]. To test the involvement of an NO effect in our model, we assessed the effect of NO supplementation in $Spr^{-/-}$ mice via treatment with diethylenetriamine NONOate ($Spr^{-/-}$/NO) [29]. NO supplementation failed to rescue the abnormalities of $Spr^{-/-}$ mice, including growth retardation (Fig. 6A), mitochondrial protein expression (Fig. 6B), OCR (Fig. 6C), membrane potential (Fig. 6D), and ROS production (Fig. 6E). Additionally, we tested whether treatment with the NOS inhibitor L-NAME inhibited the effect of BH4 supplementation on mitochondrial and cardiac functions [30]. The beneficial effects of BH4 supplementation on mitochondria and heart were not attenuated by L-NAME treatment (Fig. 6F–I). We also compared cardiac mitochondrial function between WT and eNOS$^{-/-}$ mice, but no significant mitochondrial differences were observed (Fig. 6J–N). These results suggest that mitochondrial dysfunction in $Spr^{-/-}$ mice is primarily due to BH4 deficiency independent of NO.

3.6. Increased transcription and translation of PGC1α by BH4 supplementation

To identify the molecular mechanism of BH4-mediated mitochondrial biogenesis and functional regulation, we tested whether BH4 regulates transcription or translation of PGC1α, a master regulator of mitochondrial biogenesis and OXPHOS. BH4 supplementation markedly enhanced mRNA expression of *Ppargc1a*, *Ndufs1*, *Tfam*, and *Sod2*, which were significantly reduced in $Spr^{-/-}$ mice (Fig. 7A), indicating that BH4 activates mitochondrial biogenesis and OXPHOS at the gene transcription level. We further examined the expression of major regulators of mitochondrial biogenesis and OXPHOS at the protein level and found that PGC1α, mtTFA, ERRα, and NDUFS1 levels in $Spr^{-/-}$ hearts were markedly decreased, whereas BH4 supplementation recovered the expression of these proteins (Fig. 7B). BH4 supplementation not only recovered protein levels under a pathological condition but also enhanced the expression levels of PGC1α, NRF1, and mtTFA under a healthy condition (Fig. 7C). As PGC1α regulates enzyme systems involved in ROS scavenging [31], we measured protein expression levels of major mitochondrial antioxidant proteins, including peroxiredoxin 3 (Prx3), superoxide dismutase 2 (SOD2), and glutathione peroxidase 1 (Gpx1), and found that Prx3 and SOD2 were decreased in $Spr^{-/-}$ mice. Notably, BH4 treatment rescued Prx3 and SOD2 expression but not Gpx1 expression (Fig. 7D).

The loss of mitochondria function in whole-body KO mice could be affected by various neurohormonal factors including dopamine or

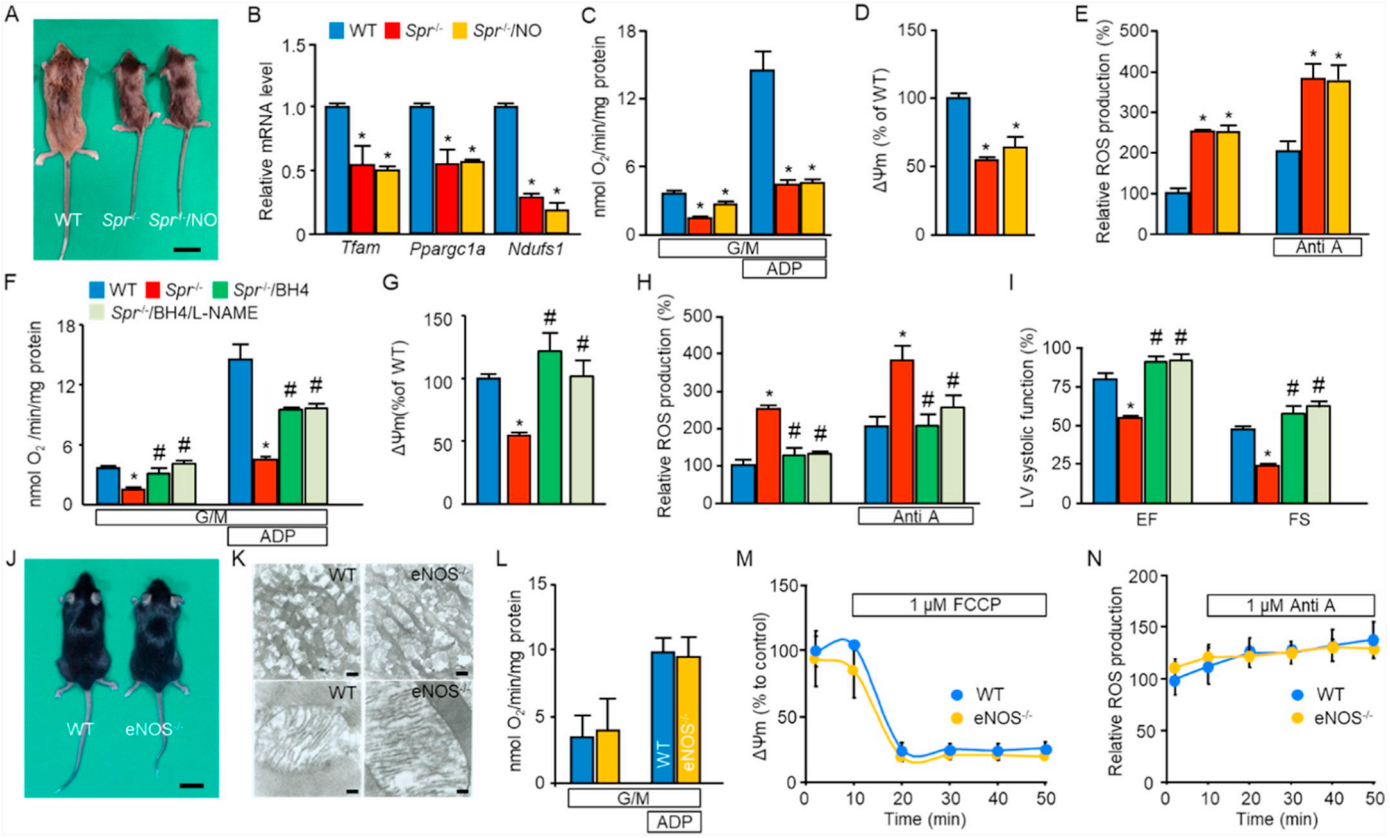

Fig. 6. No effect of NO supplementation on mitochondrial dysfunction in *Spr*$^{-/-}$ mice. (A) Phenotypic characterization (scale bar: 1 cm). (B) Relative mRNA expression ratio of selected genes. (C) Relative OCR of isolated cardiac mitochondria. (D) Relative mitochondrial membrane potential (ΔΨm). (E) Basal and antimycin A (Anti-A)-induced ROS level in isolated cardiac mitochondria. (F) Relative OCR of isolated cardiac mitochondria. (G) Relative ΔΨm. (H) Basal and Anti-A-induced ROS level in isolated cardiac mitochondria. (I) Left ventricular contractility. (J) Phenotypic characterization (scale bar: 1 cm). (K) Mitochondrial morphology (scale bars, top: 1 μm, bottom: 100 nm). (L) OCR. (M) Relative ΔΨm. (N) Relative ROS production. Data are expressed as mean ± SEM. *$p < 0.05$ vs. WT, #$p < 0.05$ vs. *Spr*$^{-/-}$, $n = 5$ mice/group, ANOVA with Bonferroni post hoc tests (B–L), two-way ANOVA with Bonferroni post hoc tests (M, N).

tyrosine hydroxylase, as BH4 is an essential conversion cofactor for these proteins [4]. To test whether the observed cardiac mitochondrial dysfunction was a direct result of BH4 deficiency or arose from systemic modulation, we assessed mitochondrial function and proteomic alterations in mouse cardiac HL-1 cells with knocked-down SPR (shSpr). After this silencing treatment, we confirmed reduced Spr mRNA levels and BH4 levels with quantitative real-time PCR and HPLC, respectively (Fig. 7E). Similar to the in vivo mouse model, shSpr cells showed lower protein levels of PGC1α, mtTFA, and NDUFS1. Twenty-four hours of BH4 supplementation (20 μM) successfully recovered the expression of all tested proteins (Fig. 7F).

Another important role of PGC1α in cardiac and skeletal muscle is the regulation of free fatty acid utilization via transcriptional regulation of CD36 and carnitine palmitoyltransferase 1 (CPT1) as well as the determination of muscle fiber type [32,33]. BH4 deficiency reduced expression of CD36 and CPT1 in both heart and skeletal muscle and reduced expression of troponin I, a marker of mitochondria-enriched slow-twitch muscle fibers, in skeletal muscle (Supplementary Fig. 2).

These results suggest that BH4 regulates transcription of PGC1α and metabolism regulatory proteins including NRF-1, ERRα, and mtTFA (mitochondrial biogenesis and OXPHOS) and Prx3 and MnSOD (antioxidant system), which collectively regulate cardiac energy metabolism (Fig. 7G).

4. Discussion

The aim of this study was to determine the biological role of BH4 in the regulation of cardiac energy metabolism. We demonstrated, for the first time, that chronic BH4 deficiency disrupts transcription of PGC1α and related energy metabolism-regulating genes involved in mitochondrial biogenesis (NRF-1, ERRα, and mtTFA) and the antioxidant system (Prx3 and MnSOD), causing severe mitochondrial and cardiac dysfunction.

BH4 deficiency led to morphological and functional defects in the hearts of transgenic *Spr*$^{-/-}$ mice. Because the heart has a high energy demand, proper ATP generation via mitochondrial oxidative phosphorylation is necessary to maintain dynamic cardiac activity. In this context, the contractile dysfunction in *Spr*$^{-/-}$ mice might reflect abnormal cardiac mitochondrial function. Although our previous study suggests that BH4 deficiency impairs mitochondrial function in *Dictyostelium discoideum* in an eNOS-independent manner [6], the underlying mechanism was unclear. However, the present multiple proteomics and systemic analysis approach revealed a strong correlation between BH4 and mitochondrial OXPHOS.

Consistent with the results of proteomics, *Spr*$^{-/-}$ mice showed reduced mitochondrial biogenesis with impaired OXPHOS function as demonstrated by ΔΨm depolarization, suppressed oxygen consumption, decreased ATP production, and increased oxidative stress. OXPHOS complex I activities were significantly suppressed as shown by reduced expression of NDUFS1, a representative subunit of complex I, in mitochondria of *Spr*$^{-/-}$ mice. Mutation or deficiency in complex I is the most common respiratory chain defect and increases susceptibility to oxidative stress, suggesting that it could be a primary target in BH4 deficiency [34,35].

Together, the results of BH4, NONOate, and L-NAME supplementation clarify that the biological role of BH4 in mitochondrial

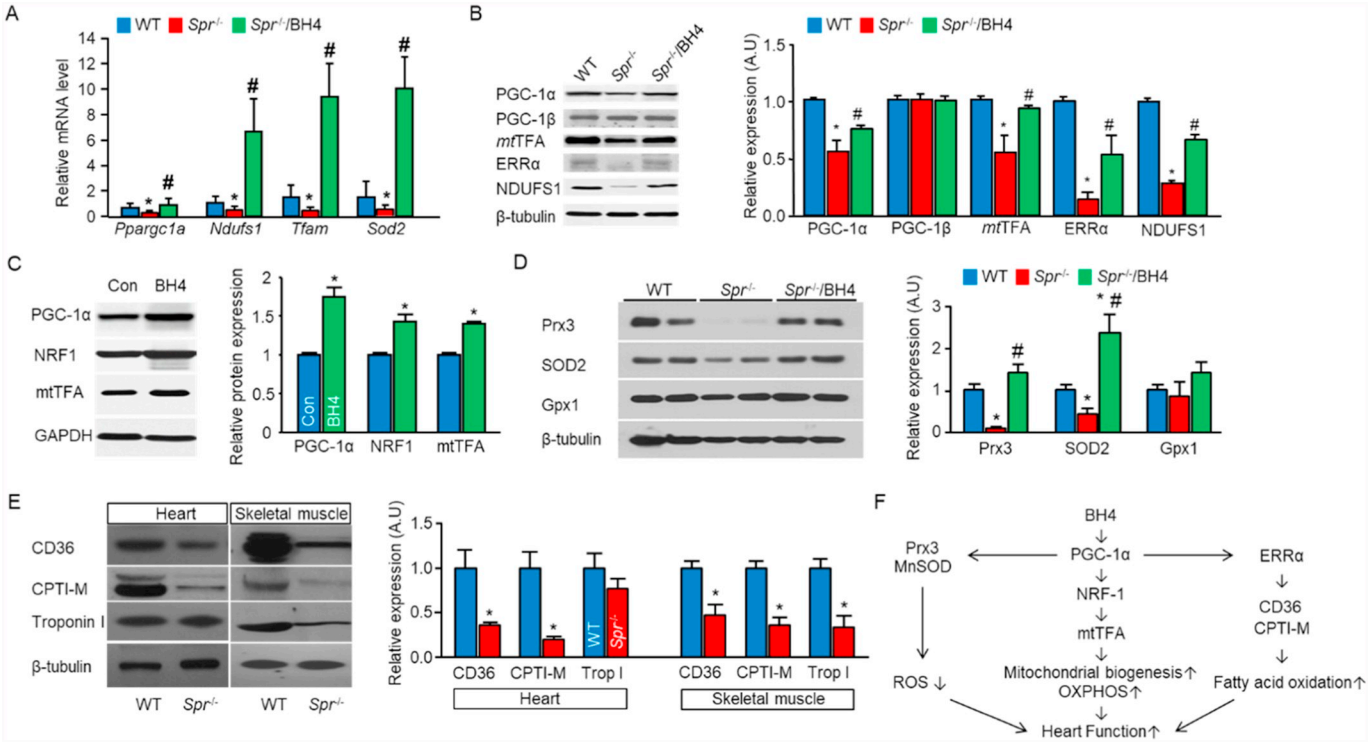

Fig. 7. Inreased transcription of PGC1α and mitochondrial metabolism regulatory proteins by BH4 supplementation. (A) Relative mRNA level of selected genes in the heart. (B) Representative immunoblots of mitochondrial biogenesis- and OXPHOS-related proteins and relative expression levels. β-tubulin was used as an internal control. (C) Representative immunoblots of selected proteins and relative expression level in WT (Con) and BH4-treated WT mice. GAPDH was used as an internal control. (D) Representative immunoblots of antioxidant proteins and relative expression levels. β-tubulin was used as an internal control. (E) Relative *SPR* mRNA level and BH4 concentration in control (shCon) and *SPR*-silenced HL-1 cells (sh*Spr*). (F) Protein expression levels of PGC1α, mtTFA, and NDUFS1. (G) Schematic diagram of mechanisms. *$p < 0.05$ vs. WT, #$p < 0.05$ vs. $Spr^{-/-}$, $n = 3$ experiments, ANOVA followed by Bonferroni post hoc tests (A, B, D), Student's *t*-tests (E, F).

biogenesis and cardiac metabolism is NO-independent. BH4 couples with eNOS to produce NO. However, unlike in other tissues, eNOS is not involved in basal mitochondrial biogenesis in the heart [28]. When we treated $Spr^{-/-}$ mice with diethylenetriamine NONOate, we found that this NO supplementation failed to rescue their abnormalities. Likewise, inhibition of NOS via treatment with L-NAME did not abolish the beneficial effects of BH4 supplementation on mitochondrial and cardiac functions. In addition, cardiac mitochondrial function was similar between WT and eNOS KO mice. Consistent with these findings, recent studies suggest an NO-independent role of BH4 in cardiovascular and neuronal systems [6,7,36,37].

As an underlying mechanism of BH4-mediated mitochondrial biogenesis and functional regulation, we found that BH4 regulated expression levels of PGC1α, ERRα, and mtTFA, which are key transcriptional regulators of mitochondrial biogenesis and oxidative phosphorylation [38,39]. BH4 deficiency decreased levels of PGC1α mRNA and protein by approximately 90% and 50%, respectively. Importantly, BH4 treatment almost completely restored PGC1α expression to a level similar to that in WT mice. The observed $Spr^{-/-}$ mitochondrial and cardiac phenotypic dysfunctions were similar to those of cardiac- and skeletal muscle-specific PGC1α/β-null mice [40]. Although decreased PGC1α is a common signature of acquired cardiac disease, mice deficient in PGC1α or β alone do not exhibit an overt cardiac phenotype under normal conditions [40]. However, these mice showed strong sensitivity to oxidative stress, hypertrophic stimulation, and aging and readily developed cardiac dysfunction [41]. ERRα is an important regulator of energy metabolism and induces expression of genes with roles in fatty acid oxidation, the TCA cycle, oxidative phosphorylation, and mitochondrial biogenesis [42]. Also, PGC1α regulates the activity and transcription of ERRα [42]. Consistently, we found reduced levels of ERRα, SOD2, CD36, and CPT1 proteins along with reduced PGC1α levels in $Spr^{-/-}$ mice. Thus, our results suggest that reduced levels of PGC1α, ERRα, and mtTFA collectively impair normal mitochondrial biogenesis and OXPHOS, which exacerbated BH4 deficiency-induced oxidative stress in $Spr^{-/-}$ mice. In addition to its role in mitochondrial biogenesis, PGC1α is a multifunctional protein that regulates transcription of antioxidant and free fatty acid utilization proteins [31,32]. Thus, we hypothesize that BH4 deficiency reduced the expression of downstream targets of PGC1α, including ERRα Prx3, SOD2, CD36, and CPT1. Reduced levels of these proteins were associated with impairments in the antioxidant system and energy metabolism in $Spr^{-/-}$ mice, which disrupted mitochondrial and cardiac functions. Furthermore, by decreasing levels of troponin I, a marker of mitochondria-enriched slow-twitch muscle fibers, BH4 deficiency may affect muscle fiber type determination and weaken physical activity via the PGC1α signaling pathway [33].

Together, our results suggest that BH4 regulates transcription of PGC1α and metabolism regulatory proteins, including NRF-1 and mtTFA (mitochondrial biogenesis and OXPHOS), Prx3 and MnSOD (antioxidant system), and ERRα, CD36, and CPTI-M (fatty acid oxidation), which collectively regulate cardiac energy metabolism. Accumulating evidence suggests that mitochondria are promising therapeutic targets in heart failure, with the recovery of PGC1α-mediated energy metabolism being a key target of mitochondria-targeted therapy [2]. Thus, our findings indicate that BH4 may have therapeutic potential for treating heart failure by enhancing mitochondrial function via transcriptional regulation of PGC1α.

Despite its beneficial effects on various cardiovascular diseases in animal models, in clinical settings, BH4 has been mainly used for patients with hyperphenylalaninemia, a genetic disorder involving total biopterin and BH4 deficiency [4]. Recent clinical studies suggest that the ratio of BH4/BH2 (i.e., reduction and oxidation forms of BH4,

respectively) is an important marker of non-genetic cardiovascular diseases, including hypertensive type-2 diabetes [43] and coronary artery disease [5]. In particular, hearts from patients with coronary artery disease exhibit normal *GCH1* and *QDPR* expression but decreased BH4 levels and BH4/BH2 ratios, suggesting the importance of non-transcriptional regulation of BH4 synthesis [5]. This clinical evidence could encourage the application of BH4 to treat various cardiovascular diseases. Our results suggest that BH4 treatment improves cardiac function not only by enhancing eNOS signaling but also by altering PGC1α-mediated mitochondrial metabolism.

5. Conclusion

In conclusion, our results demonstrate a prominent role for and underlying mechanisms of BH4 in the regulation of heart function and cardiac mitochondrial homeostasis. BH4 deficiency may be a risk factor for cardiac dysfunction, and the maintenance of optimal BH4 levels has therapeutic potential for cardiovascular diseases associated with mitochondrial dysfunction.

Supplementary data to this article can be found online at https://doi.org/10.1016/j.bbadis.2019.07.018.

Author contributions

H.K.K., J.J., S.K., B.N., Y.S.P., and J.H. contributed to the study design. H.K.K. contributed to the mitochondria functional analysis. I-S.S., S.H.J., L.T.L., M. K., and V.T.T. contributed to the study design and carried out the biochemical and enzymatic assays. T.H.K. and I.S. contributed to the echocardiography experiment. J.J., J-S.Y., J-M.A., J-Y.C., N-C. H. and S.K. contributed to the proteomics and computational analyses. N.K., M.S.K., K.S.K., and B.D.R. contributed to the immunohistochemical analysis and interpretation of echocardiography data. Y.S.P. contributed to the development of $Spr^{-/-}$ mice. I.S. and T. M contributed to the comprehension of clinical importance. Y.S.P., S.K., B.N., and J.H. supervised the study. H.K.K. and J.J wrote the manuscript. All authors discussed the results and commented on the manuscript.

Transparency document

The Transparency document associated with this article can be found, in online version.

CRediT authorship contribution statement

Hyoung Kyu Kim:Conceptualization, Methodology, Writing - original draft.**Jouhyun Jeon**:Conceptualization, Methodology, Writing - original draft.**In-Sung Song**:Investigation.**Hae Jin Heo**:Investigation.**Seung Hun Jeong**:Investigation.**Le Thanh Long**:Investigation.**Vu Thi Thu**:Investigation.**Tae Hee Ko**:Investigation.**Min Kim**:Investigation.**Nari Kim**:Formal analysis. **Sung Ryul Lee**:Investigation.**Jae-Seong Yang**:Investigation.**Mi Seon Kang**:Formal analysis.**Jung-Mo Ahn**:Investigation.**Je-Yoel Cho**:Formal analysis.**Kyung Soo Ko**:Investigation.**Byoung Doo Rhee**:Investigation.**Bernd Nilius**:Supervision, Writing - review & editing.**Nam-Chul Ha**:Software.**Ippei Shimizu**:Conceptualization, Writing - review & editing, Resources.**Tohru Minamino**:Data curation, Writing - review & editing.**Kyoung Im Cho**:Data curation. **Young Shik Park**:Conceptualization, Methodology, Resources. **Sanguk Kim**:Conceptualization, Methodology, Supervision.**Jin Han**:Conceptualization, Supervision, Funding acquisition, Project administration.

Declaration of competing interest

The authors declare no conflict of interest.

Acknowledgements

We thank Prof. Goo Taeg Oh (Ewha Women's University, Korea) for generously providing eNOS KO mice. This study was supported by the Priority Research Centers Program and the Bio & Medical Technology Development Program through the National Research Foundation of Korea (NRF), which is funded by the Ministry of Education, Science, and ICT (2010-0020224, 2015M3A9B6029133, 2018R1A2A3074998, 2018R1D1A1A09081767, and 2015004921).

References

[1] C.W. Yancy, M. Jessup, B. Bozkurt, J. Butler, D.E. Casey Jr., M.H. Drazner, G.C. Fonarow, S.A. Geraci, T. Horwich, J.L. Januzzi, M.R. Johnson, E.K. Kasper, W.C. Levy, F.A. Masoudi, P.E. McBride, J.J. McMurray, J.E. Mitchell, P.N. Peterson, B. Riegel, F. Sam, L.W. Stevenson, W.H. Tang, E.J. Tsai, B.L. Wilkoff, 2013 ACCF/AHA guideline for the management of heart failure: a report of the American College of Cardiology Foundation/American Heart Association Task Force on Practice Guidelines, J. Am. Coll. Cardiol. 62 (2013) e147–e239.
[2] M. Bayeva, M. Gheorghiade, H. Ardehali, Mitochondria as a therapeutic target in heart failure, J. Am. Coll. Cardiol. 61 (2013) 599–610.
[3] D.O. Okonko, A.M. Shah, Heart failure: mitochondrial dysfunction and oxidative stress in CHF, Nat. Rev. Cardiol. 12 (2015) 6–8.
[4] H.K. Kim, S.H. Ha, J. Han, Potential therapeutic applications of tetrahydrobiopterin: from inherited hyperphenylalaninemia to mitochondrial diseases, Ann. N. Y. Acad. Sci. 1201 (2010) 177–182.
[5] E. Arning, B. Lowes, M. Taylor, X. Meng, R. Schiffmann, T. Bottiglieri, Tetrahydrobiopterin concentrations in normal and coronary artery diseased heart tissue, Journal of Cardiovascular Medicine and Cardiology 3 (2016) 014–017.
[6] H.L. Kim, Y.K. Choi, H. Kim do, S.O. Park, J. Han, Y.S. Park, Tetrahydropteridine deficiency impairs mitochondrial function in Dictyostelium discoideum Ax2, FEBS Lett, 581 (2007) 5430–5434.
[7] J. Bailey, A. Shaw, R. Fischer, B.J. Ryan, B.M. Kessler, J. McCullagh, R. Wade-Martins, K.M. Channon, M.J. Crabtree, A novel role for endothelial tetrahydrobiopterin in mitochondrial redox balance, Free Radic. Biol. Med. 104 (2017) 214–225.
[8] S. Yang, Y.J. Lee, J.M. Kim, S. Park, J. Peris, P. Laipis, Y.S. Park, J.H. Chung, S.P. Oh, A murine model for human sepiapterin-reductase deficiency, Am. J. Hum. Genet. 78 (2006) 575–587.
[9] V.T. Thu, H.K. Kim, T. Long le, S.R. Lee, T.M. Hanh, T.H. Ko, H.J. Heo, N. Kim, S.H. Kim, K.S. Ko, B.D. Rhee, J. Han, NecroX-5 prevents hypoxia/reoxygenation injury by inhibiting the mitochondrial calcium uniporter, Cardiovasc Res, 94 (2012) 342–350.
[10] N. Kim, Y. Lee, H. Kim, H. Joo, J.B. Youm, W.S. Park, M. Warda, D.V. Cuong, J. Han, Potential biomarkers for ischemic heart damage identified in mitochondrial proteins by comparative proteomics, Proteomics 6 (2006) 1237–1249.
[11] C.C. Hughey, D.S. Hittel, V.L. Johnsen, J. Shearer, Respirometric Oxidative Phosphorylation Assessment in Saponin-permeabilized Cardiac Fibers, J Vis Exp (2011).
[12] M. Warda, H.K. Kim, N. Kim, J.B. Youm, S.H. Kang, W.S. Park, T.M. Khoa, Y.H. Kim, J. Han, Simulated hyperglycemia in rat cardiomyocytes: a proteomics approach for improved analysis of cellular alterations, Proteomics 7 (2007) 2570–2590.
[13] H.J. Park, B.G. Kim, S.J. Lee, S.H. Heo, J.Y. Kim, T.H. Kwon, E.B. Lee, H.M. Ryoo, J.Y. Cho, Proteomic profiling of endothelial cells in human lung cancer, J. Proteome Res. 7 (2008) 1138–1150.
[14] J. Braisted, S. Kuntumalla, C. Vogel, E. Marcotte, A. Rodrigues, R. Wang, S.-T. Huang, E. Ferlanti, A. Saeed, R. Fleischmann, S. Peterson, R. Pieper, The APEX Quantitative Proteomics Tool: generating protein quantitation estimates from LC-MS/MS proteomics results, BMC Bioinformatics 9 (2008) 529.
[15] M. Kanehisa, S. Goto, M. Hattori, K.F. Aoki-Kinoshita, M. Itoh, S. Kawashima, T. Katayama, M. Araki, M. Hirakawa, From genomics to chemical genomics: new developments in KEGG, Nucleic Acids Res. 34 (2006) D354–D357.
[16] W.C. Claycomb, N.A. Lanson, B.S. Stallworth, D.B. Egeland, J.B. Delcarpio, A. Bahinski, N.J. Izzo, HL-1 cells: a cardiac muscle cell line that contracts and retains phenotypic characteristics of the adult cardiomyocyte, Proc. Natl. Acad. Sci. 95 (1998) 2979–2984.
[17] M.A. Birch-Machin, D.M. Turnbull, Assaying mitochondrial respiratory complex activity in mitochondria isolated from human cells and tissues, Methods Cell Biol. 65 (2001) 97–117.
[18] G. Mattiasson, Analysis of mitochondrial generation and release of reactive oxygen species, Cytometry A 62 (2004) 89–96.
[19] T. Langenickel, I. Pagel, K. Hohnel, R. Dietz, R. Willenbrock, Differential regulation of cardiac ANP and BNP mRNA in different stages of experimental heart failure, Am. J. Physiol. Heart Circ. Physiol. 278 (2000) H1500–H1506.
[20] C. Zabel, L. Mao, B. Woodman, M. Rohe, M.A. Wacker, Y. Klare, A. Koppelstatter, G. Nebrich, O. Klein, S. Grams, A. Strand, R. Luthi-Carter, D. Hartl, J. Klose, G.P. Bates, A large number of protein expression changes occur early in life and precede phenotype onset in a mouse model for huntington disease, Mol. Cell. Proteomics 8 (2009) 720–734.
[21] X.H. Liu, L.J. Qian, J.B. Gong, J. Shen, X.M. Zhang, X.H. Qian, Proteomic analysis of mitochondrial proteins in cardiomyocytes from chronic stressed rat, Proteomics 4 (2004) 3167–3176.

[22] L.M. Stuart, J. Boulais, G.M. Charriere, E.J. Hennessy, S. Brunet, I. Jutras, G. Goyette, C. Rondeau, S. Letarte, H. Huang, P. Ye, F. Morales, C. Kocks, J.S. Bader, M. Desjardins, R.A. Ezekowitz, A systems biology analysis of the Drosophila phagosome, Nature 445 (2007) 95–101.
[23] T. Kislinger, B. Cox, A. Kannan, C. Chung, P. Hu, A. Ignatchenko, M.S. Scott, A.O. Gramolini, Q. Morris, M.T. Hallett, J. Rossant, T.R. Hughes, B. Frey, A. Emili, Global survey of organ and organelle protein expression in mouse: combined proteomic and transcriptomic profiling, Cell 125 (2006) 173–186.
[24] D.J. Pagliarini, S.E. Calvo, B. Chang, S.A. Sheth, S.B. Vafai, S.-E. Ong, G.A. Walford, C. Sugiana, A. Boneh, W.K. Chen, D.E. Hill, M. Vidal, J.G. Evans, D.R. Thorburn, S.A. Carr, V.K. Mootha, A mitochondrial protein compendium elucidates complex I disease biology, Cell 134 (2008) 112–123.
[25] S. Park, J.S. Yang, S.K. Jang, S. Kim, Construction of functional interaction networks through consensus localization predictions of the human proteome, J. Proteome Res. 8 (2009) 3367–3376.
[26] J.B. Pereira-Leal, E.D. Levy, S.A. Teichmann, The origins and evolution of functional modules: lessons from protein complexes, Philos. Trans. R. Soc. Lond. Ser. B Biol. Sci. 361 (2006) 507–517.
[27] T. Ide, H. Tsutsui, S. Kinugawa, H. Utsumi, D. Kang, N. Hattori, K. Uchida, K. Arimura, K. Egashira, A. Takeshita, Mitochondrial electron transport complex I is a potential source of oxygen free radicals in the failing myocardium, Circ. Res. 85 (1999) 357–363.
[28] R. Ventura-Clapier, A. Garnier, V. Veksler, Transcriptional control of mitochondrial biogenesis: the central role of PGC-1α, Cardiovasc. Res. 79 (2008) 208–217.
[29] Y. Hua, X.-Y. Huang, L. Zhou, Q.-G. Zhou, Y. Hu, C.-X. Luo, F. Li, D.-Y. Zhu, DETA/NONOate, a nitric oxide donor, produces antidepressant effects by promoting hippocampal neurogenesis, Psychopharmacology 200 (2008) 231–242.
[30] J. Bartunek, E.O. Weinberg, M. Tajima, S. Rohrbach, S.E. Katz, P.S. Douglas, B.H. Lorell, Chronic N(G)-nitro-L-arginine methyl ester-induced hypertension: novel molecular adaptation to systolic load in absence of hypertrophy, Circulation 101 (2000) 423–429.
[31] I. Valle, A. Álvarez-Barrientos, E. Arza, S. Lamas, M. Monsalve, PGC-1α regulates the mitochondrial antioxidant defense system in vascular endothelial cells, Cardiovasc. Res. 66 (2005) 562–573.
[32] Z. Luo, L. Ma, Z. Zhao, H. He, D. Yang, X. Feng, S. Ma, X. Chen, T. Zhu, T. Cao, D. Liu, B. Nilius, Y. Huang, Z. Yan, Z. Zhu, TRPV1 activation improves exercise endurance and energy metabolism through PGC-1alpha upregulation in mice, Cell Res. 22 (2012) 551–564.
[33] J. Lin, H. Wu, P.T. Tarr, C.Y. Zhang, Z. Wu, O. Boss, L.F. Michael, P. Puigserver, E. Isotani, E.N. Olson, B.B. Lowell, R. Bassel-Duby, B.M. Spiegelman, Transcriptional co-activator PGC-1 alpha drives the formation of slow-twitch muscle fibres, Nature 418 (2002) 797–801.
[34] D.M. Kirby, M. Crawford, M.A. Cleary, H.H. Dahl, X. Dennett, D.R. Thorburn, Respiratory chain complex I deficiency: an underdiagnosed energy generation disorder, Neurology 52 (1999) 1255–1264.
[35] A. Musatov, N.C. Robinson, Susceptibility of mitochondrial electron-transport complexes to oxidative damage. Focus on cytochrome c oxidase, Free Radic. Res. 46 (2012) 1313–1326.
[36] T. Hashimoto, V. Sivakumaran, R. Carnicer, G. Zhu, V.S. Hahn, D. Bedja, A. Recalde, D. Duglan, K.M. Channon, B. Casadei, D.A. Kass, Tetrahydrobiopterin protects against hypertrophic heart disease independent of myocardial nitric oxide synthase coupling, J. Am. Heart Assoc. 5 (2016) e003208.
[37] I. Cook, T. Wang, T.S. Leyh, Tetrahydrobiopterin regulates monoamine neurotransmitter sulfonation, Proc. Natl. Acad. Sci. U. S. A. 114 (2017) E5317–E5324.
[38] M.B. Hock, A. Kralli, Transcriptional control of mitochondrial biogenesis and function, Annu. Rev. Physiol. 71 (2009) 177–203.
[39] Z. Arany, H. He, J. Lin, K. Hoyer, C. Handschin, O. Toka, F. Ahmad, T. Matsui, S. Chin, P.-H. Wu, I.I. Rybkin, J.M. Shelton, M. Manieri, S. Cinti, F.J. Schoen, R. Bassel-Duby, A. Rosenzweig, J.S. Ingwall, B.M. Spiegelman, Transcriptional coactivator PGC-1[alpha] controls the energy state and contractile function of cardiac muscle, Cell Metab. 1 (2005) 259–271.
[40] O.J. Martin, L. Lai, M.M. Soundarapandian, T.C. Leone, A. Zorzano, M.P. Keller, A. D. Attie, D.M. Muoio, D.P. Kelly, A role for peroxisome proliferator-activated receptor gamma coactivator-1 in the control of mitochondrial dynamics during postnatal cardiac growth, in: Circ Res, vol. 114, 2014, pp. 626–636.
[41] G.C. Rowe, A. Jiang, Z. Arany, PGC-1 coactivators in cardiac development and disease, Circ. Res. 107 (2010) 825–838.
[42] J.A. Villena, A. Kralli, ERRalpha: a metabolic function for the oldest orphan, Trends Endocrinol. Metab. 19 (2008) 269–276.
[43] J. Aviles-Herrera, K.C. Arana-Pazos, L. Del, C.G.-G. Valle-Mondragon, A.F. Rubio-Guerra, Association between bh4/bh2 ratio and albuminuria in hypertensive type-2 diabetic patients, Blood pressure (mm Hg) 175 (2017) 8.8.